DOI:10.26565/2312-4334-2022-1-08 ISSN 2312-4334

CHARACTERISTICS AND OPTICAL PROPERTIES OF $Bi_2Te_{2.45}Se_{0.55}$ THIN FILM†

A.S. Salwa*, Azza El-Sayed Ahmed
Physics Department, Faculty of Science and Arts, Jouf University, Gurayat 77431, Kingdom of Saudi Arabia
Corresponding author: ssaali@ju.edu.sa
Received January 17, 2022; revised February 20, 2022; accepted March 5, 2022

Thermally evaporated $Bi_2Te_{2.45}Se_{0.55}$ thin films were examined for structural alterations and electrical conductivity. Crystallite size, micro-strain, and dislocations were all calculated using the XRD data. By using transmission electron microscopy, the morphology of thin films was investigated (TEM). The study was performed within a temperature range of (300 – 500) K. The electrical energy gap and the conductivity of the as-deposited and annealed (373, 473K) $Bi_2Te_{2.45}Se_{0.55}$ films were measured. The obtained values are (0.27, 0.26, 0.24 eV) and 3.6×10^3, 3.7×10^3 and 4.1×10^3 $ohm^{-1}.cm^{-1}$ respectively. Hall coefficient, the mean free time, the diffusion coefficient of holes, and the diffusion length, charge carrier's concentration, charge carriers' scattering mechanism, and Hall mobility were also examined. The obtained values of the charge carrier's concentration are 2.12×10^{17} -2.73×10^{17} cm^{-3}. The direct and indirect allowed energy gap decreased with increasing annealing temperature. The obtained values of indirect band gap and direct band gap ranges from 0.27- 0.24 eV and 0.375- 0.379 eV, respectively.
Keywords: Thin film; electrical properties; transmission electron microscopy; Hall Effect; optical energy gap
PACS: 32.30.Rj, 07.50.–e, 07.05.Kf, 03.65.Nk, 42.25.Bs

Recently, compounds of semiconducting chalcogenides type A_2VB_3VI (where A = Bi, Sb, and B = Te, Se) and their solid solutions are considered to be promising materials for their unique optical, electrical and magnetic properties [1-4] and concomitantly to their potential applications in solid-state thermoelectric cooling and thermoelectric generators [5-8]. The electrical, thermal conductivities and the Seebeck coefficient properties of $Bi_2(Te_{1-x}Se_x)_3$ single crystal solid solutions with x = 0.025 ($S_{2.5}$) and x = 0.05 (S_5) were studied [9]. The results showed the scattering mechanism is mainly due to acoustical phonons. Transport properties of $Bi_2Te_{2.55}Se_{0.45}$ solid solutions as a function of carrier concentration and temperature were studied [10].

J. Dheepa et al [11] studied the structural and the optical properties of thermally evaporated Bi_2Te_3 thin films. The XRD shows the hexagonal and polycrystalline structure of the focused films. The calculated lattice parameters are $a = 4.4$ Å and $C = 3.4$ Å. A. Saji et al.[12] studied the effects of fast electron bombardment and annealing on Bi_2Te_3 and $Bi_2Te_{2.9}Se_{0.1}$ single crystals. Conductivity variations from p to n-type are possible by irradiation with high-energy electrons. Koksal Yildiz et al [13] used scanning electron microscopy, SEM to examine the surface morphology and the elemental composition of the deposited film as well as a high-resolution TEM to examine the lattice image for sample $Bi_2(Te_{0.9}Se_{0.1})_3$.

In this work, the annealing temperature effect on structural properties, D.C electrical conductivity, Hall Effect and optical band gap were investigated.

EXPERIMENTAL PROCDURE

The modified Bridgeman method [2] was used to fabricate n-type almost stoichiometric single-phase polycrystalline bulk ingot materials of $Bi_2Te_{2.45}Se_{0.55}$ using the pure (99.999%) Te, Se, Bi elements enclosed in vacuum-sealed silica tubes (=10^{-4} Pa). The silica tube was placed in the hot zone of the furnace for 24 hours to melt the contents.

The tube was shaken several times during heating to ensure homogeneity. The crystallization front moved at a rate of 1.7 mm/h. The temperature of the middle zone ranges from (870 – 995) K corresponding to the crystallization temperature of the produced samples of different compositions. The consumed time to make a crystal is twelve days. The final crystal had a diameter of 1.5 cm and a length of 1.5 cm using a high vacuum coating unit, thin films were deposited on glass substrates at room temperature by conventional evaporation of synthetic solid solutions at a vacuum of 10^{-4} Pa (Edwards 306 A). During the evaporation process, the deposition rate was kept constant at 3nm/s. The film thickness was determined interferometrically as well as utilizing a quartz crystal thickness monitor (Edwards FTM4) [2]. Thin films were annealed by progressively heating them to various annealing temperatures of 373K and 473 K at a pressure of 10^{-3} Pa for two hours at each annealing temperature. After annealing, films were allowed to cool slowly to ambient temperature in a vacuum. X-ray diffractometer, XRD technique is used to verify the crystal structure of the studied material in thin films form. The morphology of the samples was examined by (TEM). Electrical conductivity, σ was measured by the conventional four-probe method using a direct current in a temperature range (300 - 500) K and Hall coefficient as well. The optical transmittance spectrum was measured using a single beam Fourier transform infrared spectrophotometer (FTIR-300E) in wavelength range (2500 – 5000) nm.

† ***Cite as***: A.S. Salwa, and A. El-Sayed Ahmed, East. Eur. J. Phys. **1**, 58 (2022), https://doi.org/10.26565/2312-4334-2022-1-08
© A.S. Salwa, A. El-Sayed Ahmed, 2022

RESULTS AND DISCUSSION

Structure analysis

Figure 1 shows the XRD patterns of the as-deposited and annealed $Bi_2Te_{2.45}Se_{0.55}$ films, it was found that the peak intensity increases appreciably with the increasing of annealing temperature. Analysis of XRD data reveals good crystallinity of films by annealing, with preferred orientation (015) at 2θ = 32.5°C. The crystallite size is calculated by Debye - Scherer equation [14]:

$$D = 0.9\,\lambda/\beta\,cos\theta \tag{1}$$

Where λ is the wavelength of CuKα radiation of XRD, β is the full width at half maximum at reflection plane (015) and θ is diffraction angle.

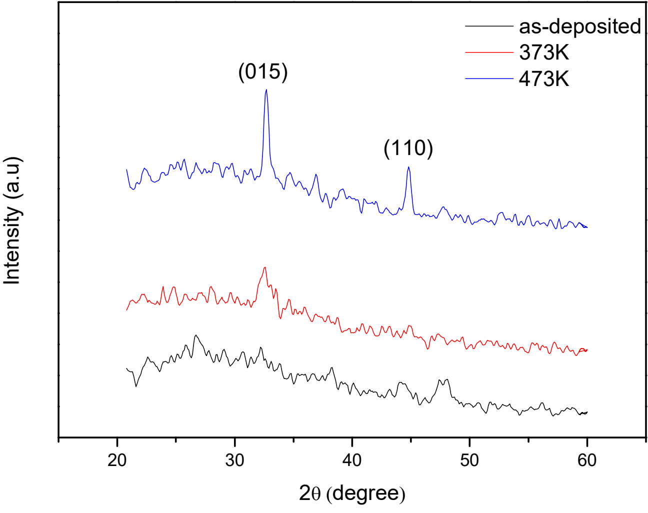

Figure 1. XRD pattern of $Bi_2Te_{2.45}Se_{0.55}$ thin films

The obtained results confirm the increasing of crystallite size with the increase of annealing temperature because of re-crystallization which leads to the reduction of deformation or defects present in the film. The annealing at (473 K) enhances the quality of the crystalline structure of $Bi_2Te_{2.45}Se_{0.55}$ films [15]. Micro-strain, S (non-uniform strain) was determined using XRD according to [16]:

$$s = \beta\cos\theta/4 \tag{2}$$

As the annealing temperature increases, the micro-strain decreases. This may be attributed to the imperfections in the crystal structure. As a result of crystallinity improvement because of annealing, the micro-strain is reduced.
The dislocation density δ is defined as the length of dislocation lines per volume unity of a crystal. δ is a significant characteristic of the structure, so it is estimated by [16]:

$$\delta = n/D^2 \tag{3}$$

where (n) is an integer number, D is the crystallite size.

As the annealing temperature increases, the dislocation density decreases as a result of the reduction of lattice defects, and consequently, the crystalline quality increases due to the modification of the periodic arrangements of atoms in their crystal lattice. This confirms the crystalline enhancement of material at 373K and 473K annealing temperature, as documented by authors [17].

The calculated values of crystallite size, micro-strain, dislocation density, and the numbers of crystallites are listed in Table 1.

Table 1. The calculated values of crystalline size from (XRD, TEM), micro-strain, and dislocations for the annealing temperature (373, 473) K for $Bi_2Te_{2.45}Se_{0.55}$ thin film.

Ta (K)	Crystalline Size XRD D (nm)	Crystalline Size TEM D (nm)	Micro-strain $S\times10^{-3}$	Dislocation density (Line/m^2) $\delta\times10^{14}$
373	43	45	7.95	5.27
473	75	80	4.61	1.76

Morphology analysis of $Bi_2Te_{2.45}Se_{0.55}$ thin film

Figure 2(a,b,c) shows a TEM image of the as-deposited and annealed $Bi_2Te_{2.45}Se_{0.55}$ thin films. As seen in Figure 2a, the as-deposited film has a rough surface with irregular crystallite size. The morphology of the annealed films at 373 K does not change much but the crystallite size uniformity improved as shown in Figure 2b. Additionally, the annealed films at 473K have a continuous and homogeneous surface as observed in Figure 2c.

From TEM analysis, the crystallite size was around 45 nm and 80 nm for different annealed temperatures (373 K and 473 K) respectively. This result is matched with the data obtained from the XRD diffraction method.

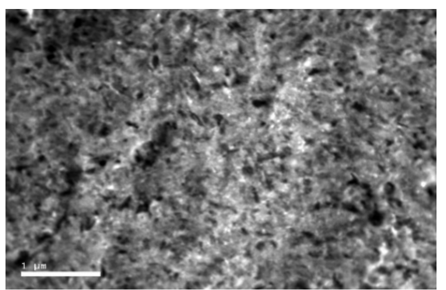

Figure 2a. Transmission electron microscopy images of the as-deposited $Bi_2Te_{2.45}Se_{0.55}$ thin film.

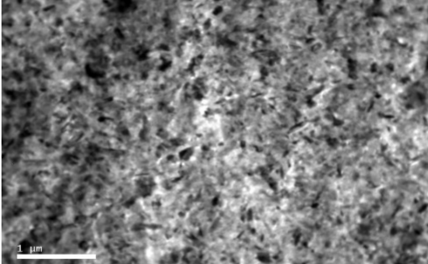

Figure 2b. Transmission electron microscopy images of $Bi_2Te_{2.45}Se_{0.55}$ thin films at Ta = 373K.

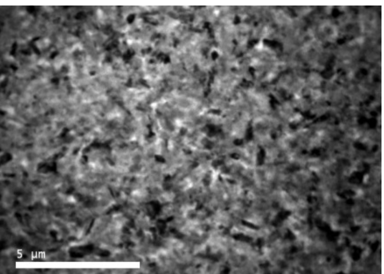

Figure 2c. Transmission electron microscopy images of $Bi_2Te_{2.45}Se_{0.55}$ thin film at Ta = 473K.

Annealing effect of electrical conductivity

Figure 3 shows the results of the temperature dependence of the electrical conductivity of the as-deposited and that annealed $Bi_2Te_{2.45}Se_{0.55}$, thin films at 373, 473K for two hours

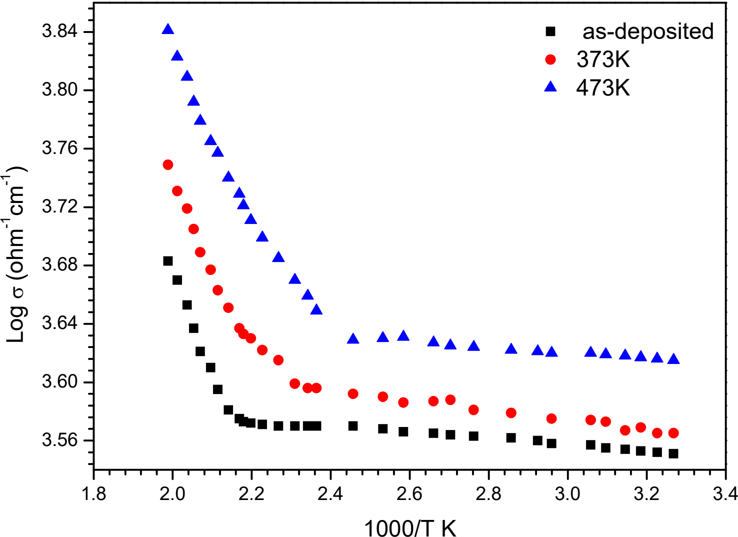

Figure 3. The temperature dependence of electrical conductivity Log σ for the deposited thin films and annealed $Bi_2Te_{2.45}Se_{0.55}$ films.

One can confirm that the as-deposited and annealed films at 373,473 have a semiconductor behavior. The curve consists of three regions; the first region in the temperature range (300-385) K and σ finishes in the extrinsic region. The conductivity shows a slightly increase in the low- temperature range due to the release of ionized acceptors and their transition from the impurity level. The second region refers to the transition region, where the behavior of s is influenced by the charge carrier's concentration as well as its mobility. A rapid linear rise in conductivity is observed within the third region at high temperatures of over 400 K. This result demonstrates that, at the high temperature region, both electrons and holes contribute to conductance. By annealing temperature, the conductivity (σ) increases. The conductivity at room temperature for the as-deposited sample and annealed temperature 373, 473K are 3.6 $x10^3$, 3.7 $x10^3$, and $4.1x10^3$ ohm^{-1} cm^{-1} respectively.

This increase in conductivity by annealing may be attributed to the improvement of crystallite size and a decrease of defects' number which allows more carriers to flow through the system to take part in conduction [18]. These results confirm the structural investigations by X-ray, which indicates the increase of crystallinity of the films by annealing. This agrees well with the results of other works for chalcogenide materials [18].

The temperature dependence of electrical conductivity was investigated using Arrhenius equation [19]:

$$\sigma = \sigma_o exp(-\Delta E_g/2KT) \quad (4)$$

The measured d.c electrical conductivity indicates two straight lines with different slopes, both could fit the relation. The conduction mechanism due to carriers excited into localized states at the edge of the band by hopping at low temperatures (300 - 400) K, and the conduction mechanism due to carriers excited into extended states beyond the mobility edge by thermal excitation at higher temperatures (400-500) K. The activation energy calculated from the first line is in the temperature range 300 - 400K, while the energy gap calculated from the other line within temperature range 400-500K. The values of energy gap and activation energy are tabulated in a table (2). This agrees well with the results of other works for chalcogenide materials [19].

Table (2) Values of energy gap and activation energy.

Ta (K)	$E_g(\sigma)$ e.v 400-500K	$\Delta E(\sigma)$ e.v 300-400K
473	0.24	7.74×10^{-3}
373	0.26	7.94×10^{-3}
As-deposited	0.27	9.02×10^{-3}

Hall Effect analysis

Hall measurements are an important tool for the characterization of materials, particularly semiconductors so Hall coefficient, R_H of the as-prepared and annealed $Bi_2Te_{2.45}Se_{0.55}$ films is measured and depicted in Fig. 4. It is clear that curves have the same trend at different annealing temperatures. Besides, the results indicate that the samples have p-type conduction because of the positive sign of R_H values so that the majority of carriers are holes.

At room temperature, R_H has a positive value range from (29.5 - 23.9) cm^3/C for as-deposited and annealed films.

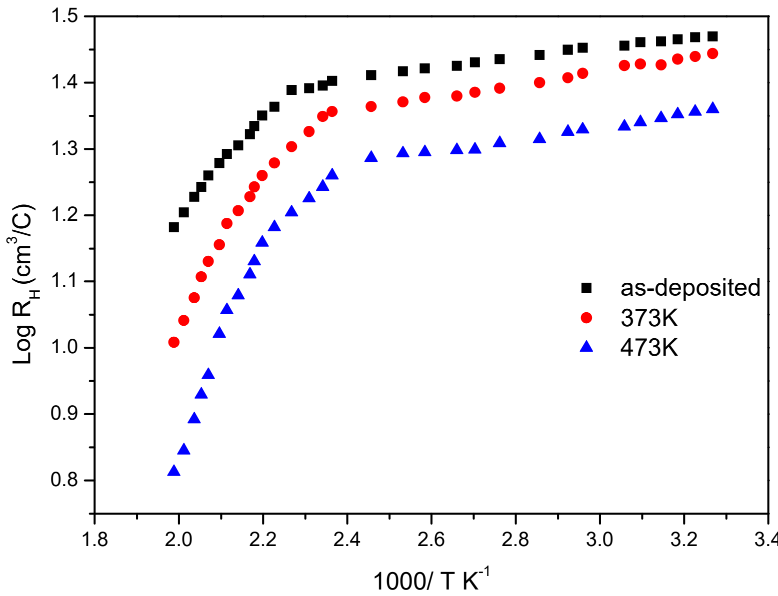

Figure 4. The temperature dependence of Log R_H Vs 1000/T(k) for the as-deposited and annealed $Bi_2Te_{2.45}Se_{0.55}$ films.

The charge carrier's concentration is estimated by equation:

$$P = 1/e\, R_H \quad (5)$$

And the concentration of charge carriers at a room temperature range from 2.12×10^{17} to 2.73×10^{17} cm^{-3} for as-deposited and annealed films. The increase of charge carriers with annealing temperature is due to the crystalline enhancement of the material. Figure 5 shows the temperature dependence of carrier concentration calculated by:

$$P = C \exp(-\Delta E_g/2K_\beta T) \quad (6)$$

Within the temperature range of (300 – 400) K, the number of free carrier P increases slightly with increasing temperature, suggesting ionization of the impurity centers whereas the number of free carriers increased sharply as the temperature rises to 400 K refers to intrinsic conduction. The energy gap can be computed from the slope of the curve within the temperature range (400- 500) K through the intrinsic region. It was (0.24 - 0.264) eV for as-deposited and annealed films. The acceptor levels energy above the top of the valence band in the extrinsic region (300-400) K

ranging from (7.69×10^{-3} – 8.9×10^{-3}) for as-deposited and annealed films. The values of energy gap and energy of acceptor level are closed to that obtained from electrical conductivity measurements.

Fig. 5 shows the temperature dependence of charge carrier concentration Log P of as-deposited thin films and annealed $Bi_2Te_{2.45}Se_{0.55}$ films.

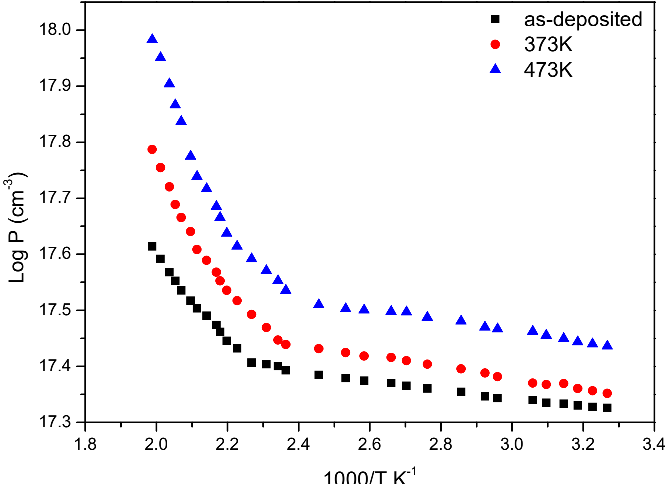

Figure 5. The temperature dependence of charge carrier concentration Log P Vs 1000/T(k) for the as- deposited and annealed $Bi_2Te_{2.45}Se_{0.55}$ films.

By using the data of R_H and conductivity, the charge carrier's mobility can be evaluated by the relation:

$$\mu_H = \sigma R_H` \tag{7}$$

The temperature dependence of Hall mobility is shown in figure 6. The curve is divided into two regions at the transition temperature of 440K.

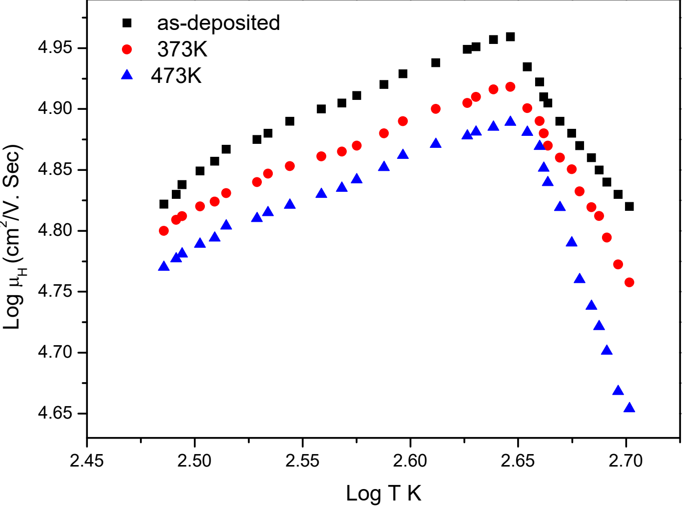

Figure 6. The temperature dependence of Hall mobility Log μ_H Vs log/T(k) for the as-deposited and annealed $Bi_2Te_{2.45}Se_{0.55}$ films.

The presence of two different types of modes on mobility variation around the transition temperature, 440K, can be seen in figure 6. At low-temperature T < 440 K, the mobility increases by the increase of temperature obeying $T^{2.4}$. The ionized impurities scattering mechanism [20, 21] is dominant for T < 440 K. At the region T ≥ 440 K, the carrier's mobility decreases by the increasing of temperature obeying $T^{-1.4}$. The lattice scattering mechanism [22] is dominant in this region. The mobility of $Bi_2Te_{2.45}Se_{0.55}$ increases by increasing the annealing temperature is due to the enhancement of the crystallinity. The diffusion coefficient of holes can be determined using the assumption that the effective mass of holes is equal to the rest mass:

$$D_p = (KT/e)\,\mu_p \tag{8}$$

The computed values of the diffusion coefficient at room temperature are (1962.8 – 1523.6) $cm^2.sec^{-1}$ for as-deposited and annealed films. In addition, the mean free time of hole estimated according to:

$$\tau_p = \mu_p m/e \quad (9)$$

The obtained values are (1.11×10^{-12} – 0.86×10^{-12}) sec for as-deposited and annealed films. The diffusion length of holes L_p was calculated at room temperature for as-deposited and annealed films and its values are (7×10^{-11} – 8×10^{-11}) cm.

Optical analysis

The knowledge of the optical characteristics of materials is important in the design and analysis of the optoelectronic devices.

The optical transmittance spectrum T of the as-deposited and annealed films were measured at room temperature within wavelength range (2500-5000) nm using Fourier transform infrared (FTIR) as shown in Figure 7.

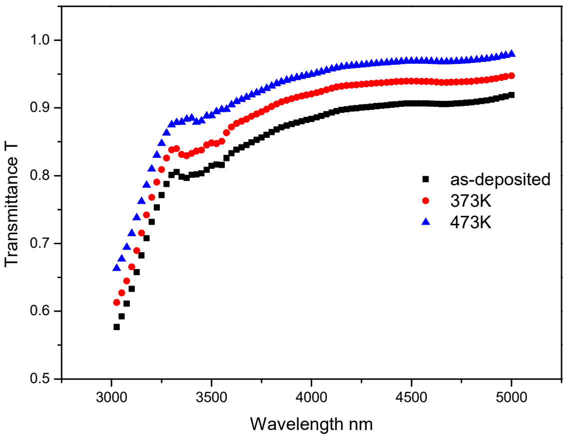

Figure 7. Transmittance spectrum versus wavelength for the as-deposited and annealed $Bi_2Te_{2.45}Se_{0.55}$ films.

It is clear that the transmittance increase by increasing temperature. The average value of transmittance increases from 90% to 99% with annealing temperature. The absorption edges shift toward higher values of wavelength with increasing the annealing temperatures. The increase of transmittance spectra with increasing annealing temperature attributed to the enhancement of the crystallinity of films [17].

The absorption coefficient calculated using:

$$\alpha = {}^{1}/_{d}\, Ln\left({}^{1}/_{T}\right) \quad (10)$$

Where α is absorption coefficient, d is a film thickness and T optical transmittance.
In the high absorption region, the optical band gap can be determined by Tauc model [17].

$$\alpha h\nu = B\left(h\nu - E_g\right)^n \quad (11)$$

Where B is a constant, $h\nu$ the photon energy, E_g the optical band gap and n is a number refer to the optical transition type (1/2, 2/3, 2, 3) for direct allowed transition, direct forbidden transition, indirect allowed transition and indirect forbidden transition, respectively. Figure 8 represent the variation of $(\alpha h\nu)^{0.5}$ as a function of photon energy$(h\nu)$. The indirect energy gap can be computed from the extrapolating straight line with photon energy axis. The energy gap decreases with increase of annealed films from 0.27 - 0.24 eV as a result of enhancement of film's crystallinity. These results match with data obtained by electrical and Hall measurements.

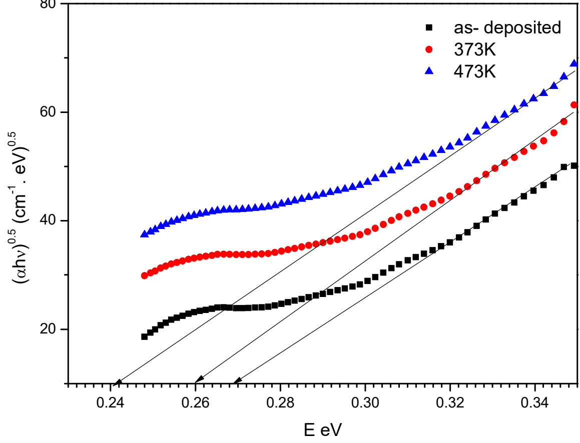

Figure 8. Plot $(\alpha h\nu)^{0.5}$ versus of photon energy(E) for the as-deposited and annealed $Bi_2Te_{2.45}Se_{0.55}$ films.

Figure 9 describes $(\alpha h\nu)^2$as a function of photon energy. The direct allowed band gap can be determined by extrapolating straight line with photon energy axis. The values of direct allowed and indirect allowed energy gap record in table 3.

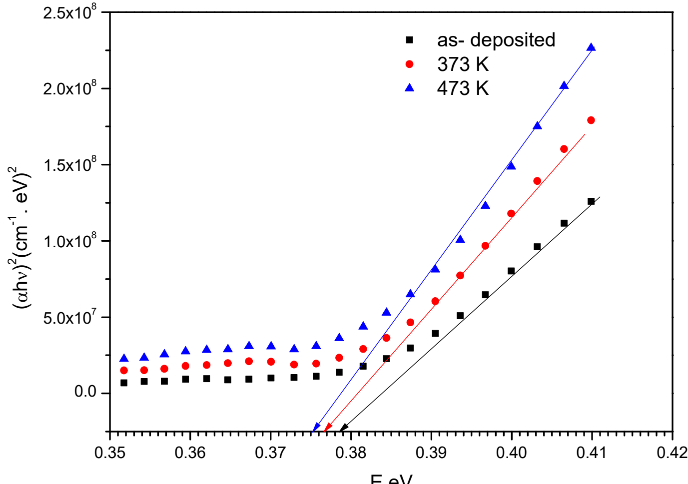

Figure 9. Plot $(\alpha h\nu)^2$ versus of photon energy(E) for the as-deposited and annealed $Bi_2Te_{2.45}Se_{0.55}$ films.

Table 3. Optical energy gap values for the as-deposited and annealed $Bi_2Te_{2.45}Se_{0.55}$ films.

Ta(K)	E_g^{ind}e.v	E_g^de.v
473	0.24	0.375
373	0.259	0.377
As-deposited	0.272	0.379

CONCLUSION

The effect of thermal annealing at (373, 473K) on the physical properties of $Bi_2Te_{2.45}Se_{0.55}$ films has been studied. The as-deposited and the annealed thin films have a rhombohedral structure. Crystalline size, micro-strain, and dislocation density were calculated at 373, 473K annealing temperature.

The electrical conductivity has been measured in the temperature range 300- 500K.

The measurements have been done for the as-deposited and annealed films (373, 473K). The conductivity of the as-deposited and annealed films varies with temperature it shows conductivity enhancement as a function of annealing.

The Hall coefficient has been measured in the temperature range 300-500K for the as-deposited and annealed films (373, 473K) where the charge carrier's concentration was calculated. The scattering mechanism is classified into two kinds, at low temperature the scattering mechanism dominant acoustical phonon while, at high temperature the scattering mechanism dominant ionized impurities. In addition, the mean free time, the diffusion coefficient of holes, and the diffusion length were computed. The optical energy gap calculated for as-deposited and annealed films. The values of direct allowed and indirect allowed energy gaps were decreased by increasing of annealing temperature. This behavior is attributed to the enhancement of the films crystalllinity.

Funding. The authors did not receive any support from any organization for the submitted work.

Conflict of interest. The authors declare that they have no conflict of interest.

ORCID IDs

A.S. Salwa, https://orcid.org/0000-0003-4000-4754; **Azza El-Sayed Ahmed**, https://orcid.org/0000-0002-5389-4111

REFERENCE

[1] D. Arivuoli, F.D. Gnanam, P. Ramasamy, Growth and microhardness studies of chalcogneides of arsenic, antimony and bismuth, J. Mater. Sci. Lett. **7**, 711 (1988). https://doi.org/10.1007/BF00722076
[2] L.I. Soliman, M.M. Nassary, H.T. Shaban, A.S. Salwa. Influence of Se on the electron mobility in thermal evaporated $Bi_2(Te_{1-x}Se_x)_3$ thin films, Vacuum, **85**, 358 (2010). https://doi.org/10.1016/j.vacuum.2010.06.003
[3] D. Qian, Z. Ye, L. Pan, Z. Zuo, D. Yang, and Y. Yan, The Mechanical and Thermoelectric Properties of Bi2Te3-Based Alloy Prepared by Constrained Hot Compression Technique, Metals, **11**, 1060, (2021). https://doi.org/10.3390/met11071060
[4] D.D. Awschalom, D.P. Divincenzo, J.F. Smyth, Macroscopic quantum effects in nanometer-scale magnets, Science, **258**, 414 (1992). https://doi.org/10.1126/science.258.5081.414
[5] N. Jaziri, A. Boughamoura, J. Müller, B. Mezghani, F. Tounsi, and M. Ismail, A comprehensive review of Thermoelectric Generators: Technologies and common applications, Energy Reports, **6**, 264 (2020). https://doi.org/10.1016/j.egyr.2019.12.011

[6] G.J. Snyder, J.R. Lim, C-K. Huang, and J.P. Fleurial, Thermoelectric microdevice fabricated by a MEMS-like electrochemical process, Nat. Mater. **2**, 528 (2003). https://doi.org/10.1038/nmat943
[7] C.B. Vining, Thermopower to the people, Nature **423**, 391 (2003). https://doi.org/10.1038/423391a
[8] T.C. Harman, P.J. Taylor, M.P. Walsh, and B.E. La Forge. Quantum Dot Superlattice Thermoelectric Materials and Device. Science, **297**, 2229 (2002). https://doi.org/10.1126/science.1072886
[9] M. Carle, P. Pierrat, C. Lahalle-Gravier, S. Scherrer, and H. Scherrer, Transport properties of *n*-type $Bi_2(Te_{1-x}Se_x)_3$ single crystal solid solutions ($x \leqslant 0.05$); J. Phys. Chem. Solids, **56**, 201 (1995). https://doi.org/10.1016/0022-3697(94)00166-9
[10] C. Lahalle-Gravier, B. Lenoir, H. Scherrer, and S. Scherrer, Thermoelectric characterization of $Bi_2Te_{2.55}Se_{0.45}$ solid solution crystal. J. Phys. Chem. Solids, **59**, 13 (1998). https://doi.org/10.1016/S0022-3697(97)00119-4
[11] J. Dheepa, R. Sathyamoorthy, and A. Subbarayan, Optical properties of thermally evaporated Bi_2Te_3 thin films, Journal of Crystal Growth, 274, 100 (2005). https://doi.org/10.1016/j.jcrysgro.2004.09.070
[12] K. Yildiz, U. Akgul, H.S. Leipner, and Y. Atici, Electron microscopy study of thermoelectric n-type $Bi_2(Te_{0.9}Se_{0.1})_3$ film deposited by dc sputtering Superlattices and Microstructures 58, 60 (2013). https://doi.org/10.1016/j.spmi.2013.02.013
[13] A. Saji, and M. Elizabeth; Effects of fast electron bombardment and annealing on Bi_2Te_3 and $Bi_2Te_{2.9}Se_{0.1}$ single crystals, Semicond. Sci. Technol. **18**, 745 (2003). https://doi.org/10.1088/0268-1242/18/8/305
[14] A.S. Salwa, A. Salem, and H.T. Shaban, Linear and nonlinear optical studies of indium selenide thin films prepared by thermal evaporation technique, Optik, **241**, 166874 (2021). https://doi.org/10.1016/j.ijleo.2021.166874
[15] M.H. Kabir, M.M. Ali, M.A. Kaiyum, and M.S. Rahman, Effect of annealing temperature on structural morphological and optical properties of spray pyrolized Al-doped ZnO thin films, J. Phys. Commun. **3**, 105007 (2019). https://doi.org/10.1088/2399-6528/ab496f
[16] A.S. Salwa, and A. Salema, "Linear and nonlinear optical properties of SnS thermally evaporated thin films" Optik. **196**, 163140 (2019). https://doi.org/10.1016/j.ijleo.2019.163140
[17] A.S. Salwa, and M.S. Abd El-Sadek, Annealing temperature effect to optimize the optical properties of SnS thin films, Eur. Phys. J. Plus, 136, 696 (2021). https://doi.org/10.1140/epjp/s13360-021-01676-6
[18] T. Daniel, U. Uno, K. Isah, and U. Ahmadu, Tuning of SNS thin film conductivity on annealing in an open air environment for transistor application, East Eur. J. Phys. **2**, 94 (2020). https://doi.org/10.26565/2312-4334-2020-2-08
[19] A. Salem, and M.H. Alhossainy, Electrical conductivity and Hall effect measurements of crystalline copper indium gallium diselenide, Materials Chemistry and Physics, **263**, 124436 (2021). https://doi.org/10.1016/j.matchemphys.2021.124436
[20] C. Riha, B. Düzel, K. Graser, O. Chiatti, E. Golias, J. Sánchez-Barriga, O. Rader, O.E. Tereshchenko, and S.F. Fischer, Electrical Transport Properties of Vanadium-Doped $Bi_2Te_{2.4}Se_{0.6}$, Phys. Status Solidi B, **258**, 2000088 (2021). https://doi.org/10.1002/pssb.202000088
[21] A. Salem, A.S. Salwa, S.A. Hussein, and M. Ezzeldien, Synthesis and Electrical Transport Properties of $CuInGaTe_2$. J Laser Opt Photonics, **5**, 2 (2018). https://doi.org/10.4172/2469-410X.1000183
[22] S. Majdi, V. Djurberg, N. Suntornwipat, M. Gabrysch, and J. Isberg, Carrier Scattering Mechanisms: Identification via the Scaling Properties of the Boltzmann Transport Equation, Adv. Theory Simul. **4**, 2000103, (2021). https://doi.org/10.1002/adts.202000103

ХАРАКТЕРИСТИКИ ТА ОПТИЧНІ ВЛАСТИВОСТІ ТОНКОЇ ПЛІВКИ $Bi_2Te_{2.45}Se_{0.55}$

А.С. Салва, Азза Ель-Сайед Ахмед
Фізичний факультет, факультет науки і мистецтв, Університет Джуфа
Гураят 77431, Королівство Саудівська Аравія

Термічно випарені тонкі плівки $Bi_2Te_{2.45}Se_{0.55}$ були досліджені на предмет структурних змін та електропровідності. Розмір кристалітів, мікродеформація та дислокації були розраховані з використанням даних XRD. За допомогою просвічуючої електронної мікроскопії досліджено морфологію тонких плівок (TEM). Дослідження проводили в інтервалі температур (300–500) K. Виміряно електричний енергетичний зазор та провідність наплавлених і відпалених (373, 473 K) плівок $Bi_2Te_{2.45}Se_{0.55}$. Отримані значення (0,27, 0,26, 0,24 еВ) і 3,6×103, 3,7×103 та 4,1×103 $Ом^{-1}.см^{-1}$ відповідно. Також досліджено коефіцієнт Холла, середній вільний час, коефіцієнт дифузії дірок, довжину дифузії, концентрацію носіїв заряду, механізм розсіювання носіїв заряду та рухливість Холла. Отримані значення концентрації носіїв заряду становлять 2.12×10^{17}-2.73×10^{17} $см^{-3}$. Прямий і непрямий дозволений енергетичний зазор зменшувався з підвищенням температури відпалу. Отримані значення непрямої забороненої зони і прямої забороненої зони коливаються в межах 0,27-0,24 еВ і 0,375-0,379 еВ відповідно.

Ключові слова: тонка плівка, електричні властивості, просвічувальна електронна мікроскопія, ефект Холла, оптичний енергетичний зазор